ACS APPLIED MATERIALS & INTERFACES

Research Article

Cite This: ACS Appl. Mater. Interfaces 2019, 11, 43581−43587

www.acsami.org

Enzyme-Catalytic Self-Triggered Release of Drugs from a Nanosystem for Efficient Delivery to Nuclei of Tumor Cells

Huanan Li,*,† Qianyan Li,† Wei Hou,† Jingni Zhang,† Chenhao Yu,† Deping Zeng,§ Gang Liu,*,‡ and Faqi Li*,†

†State Key Laboratory of Ultrasound in Medicine and Engineering, College of Biomedical Engineering, and §Chongqing Key Laboratory of Biomedical Engineering, Chongqing Medical University, Chongqing 400016, Sichuan, P. R. China

‡State Key Laboratory of Molecular Vaccinology and Molecular Diagnostics & Center for Molecular Imaging and Translational Medicine, School of Public Health, Xiamen University, Xiamen 361102, Fujian, P. R. China

Supporting Information

ABSTRACT: Stimulus-responsive drug delivery nanosystems (DDSs) are of great significance in improving cancer therapy for intelligent control over drug release. However, among them, many DDSs are unable to realize rapid and sufficient drug release because most internal stimulants might be consumed during the release process. To address the plight, an abundant supply of stimulants is highly desirable. Herein, a core crosslinked pullulan-di-(4,1-hydroxybenzylene)diselenide nanosystem, which could generate abundant exogenous-stimulant reactive oxygen species (ROS) via tumor-specific NAD(P)H:quinone oxidoreductase-1 (NQO1) catalysis, was constructed by the encapsulation of *β*-lapachone. The enzyme-catalytic-generated ROS induced self-triggered cascade amplification release of loaded doxorubicin (DOX) in the tumor cells, thus achieving efficient delivery of DOX to the nuclei of tumor cells by breaking the diselenide bond of the nanosystem. As a result, the antitumor effect of this nanosystem was significantly improved in the HepG2 xenograft model. In general, this study offers a new paradigm for utilizing the interaction between the loaded agent and carrier in the tumor cells to obtain self-triggered drug release in the design of DDSs for enhanced cancer therapy.

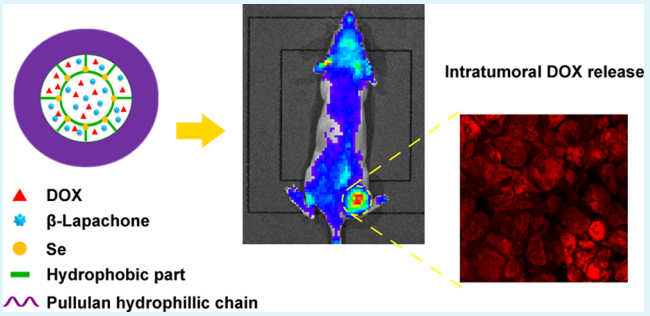

KEYWORDS: *β-lapachone, exogenous-stimulant, cascade amplification drug release, core crosslinked, cancer therapy*

1. INTRODUCTION

Cancer therapy based on nanosystems has been considered as potential alternatives to conventional chemotherapy because they could alter the pharmacokinetics and biodistribution of drugs and exert a stronger antitumor effect.[1−4] However, drug delivery nanosystems (DDSs) usually failed in realizing sufficient drug release and delivery to the nuclei of tumor cells, limiting their clinical significance.[5] Currently, many research studies focus on developing DDSs with stimulus-responsive properties.[6−8] Ye et al. reported pH-responsive micelles for the co-delivery doxorubicin (DOX)/siRNA. The nanosystem was stable in the neutral environment and could release DOX/siRNA in the acidic environment.[9] Wang et al. constructed core−shell−SS−shell-structured magnetic composite nanoparticles with a combination of PTT and DOX, which was redox-responsive in the cytoplasm and released the loaded DOX.[10] Naz et al. developed enzyme-responsive mesoporous silica nanoparticles for mitochondria multistage-targeted drug delivery.[11] Yet, many stimulus-responsive DDSs are unable to achieve rapid and sufficient drug release as internal stimulants (such as glutathione, H^+, reactive oxygen species, enzymes, etc., and their combinations[12−14]) are largely exhausted during the release process.[7,15−18] Therefore, introducing an abundant supply of exogenous stimulants to trigger drug release in the tumor cells is highly desirable.

It is reported that the NAD(P)H:quinone oxidoreductase-1 (NQO1) enzyme is overexpressed in different types of tumor cells up to 100 times.[19] *β*-Lapachone could generate reactive oxygen species (ROS) through catalysis of the NQO1 enzyme.[20,21] Ye et al. confirmed that *β*-lapachone could increase the ROS level and further overcome multidrug resistance in the tumor cells.[21] During the catalysis process, the NQO1 enzyme is not involved in the reaction and it could not be consumed and thus continuously provide stimulants during the drug release process. Therefore, using *β*-lapachone to amplify the ROS stimulant level in the tumor cells, as well as to overcome internal ROS heterogeneous distribution in the tumor tissues, helps to increase the release and nuclear delivery of the drug from ROS-responsive DDSs through cascade amplification.

Received: August 27, 2019
Accepted: October 30, 2019
Published: October 30, 2019

Downloaded via XIAMEN UNIV on February 11, 2020 at 05:45:27 (UTC).
See https://pubs.acs.org/sharingguidelines for options on how to legitimately share published articles.

© 2019 American Chemical Society

DOI: 10.1021/acsami.9b15460
ACS Appl. Mater. Interfaces 2019, 11, 43581−43587

To achieve efficient cancer therapy, successful delivery of DDSs into the tumor is just as important as sufficient drug release. Extensive studies suggested that DDSs constructed with modified polysaccharides (e.g. pullulan, chitosan, and hyaluronic acid) showed feasible stability in vivo, which contributed to traversing the tumor vessel and accumulating in the tumor tissue.[22−24] Meanwhile, in others' and our previous work, pullulan polysaccharide nanocarriers exhibited favorable stability, high drug loading capability, and hepatic targeting efficacy.[25−31]

Herein, inspired by the effect of β-lapachone to generate ROS, and based on the successful application of modified pullulan polysaccharide DDSs as well as our previous research, as shown in Figure 1, we developed a new core crosslinked

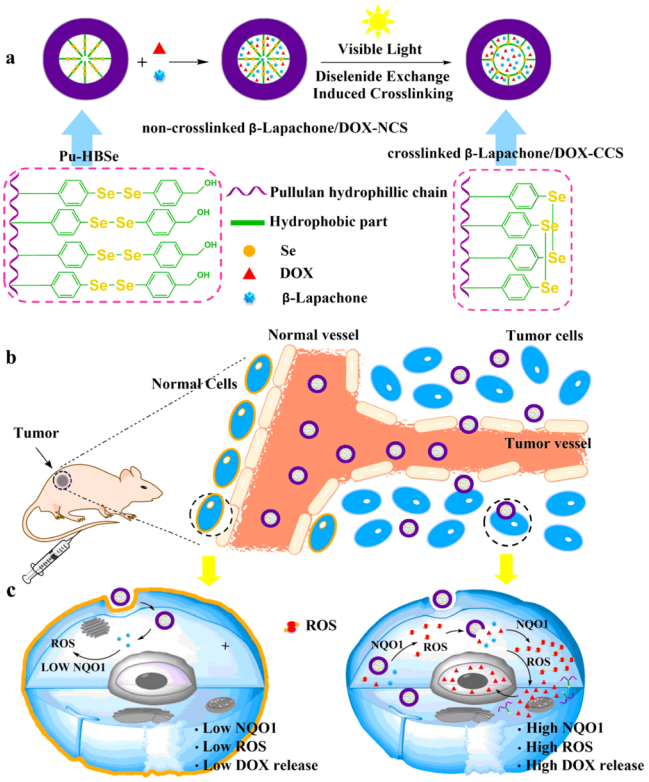

Figure 1. Schematic illustrations of the cascade amplification release process of β-lapachone/DOX-CCS in the tumor cells.

pullulan nanosystem containing diselenide bond, which was ROS-responsive and encapsulated high loading content of β-lapachone and DOX. The crosslinked nanoparticles could prevent premature drug leakage during the delivery process, thus improving drug stability in the nanosystem.[32,33] Furthermore, we explored how the cross-linking influenced the physical characteristics and the biological fate of this nanosystem. After being endocytosed by tumor cells, the nanosystem would first release a portion of β-lapachone in the presence of internal stimulants (glutathione or ROS), which could induce a significant increase of ROS via NQO1 catalysis. The generated ROS, like a kindling, could subsequently self-trigger the break of diselenide (Se−Se) bond and disintegrate the nanosystem, leading to amplified β-lapachone/DOX release like fireworks. More importantly, β-lapachone and ROS could induce cellular apoptosis,[34−36] and thus they have been considered as significant therapeutic agents. We integrated multiple mechanisms into a single nanosystem as an exciting therapeutic candidate. Therefore, this design might achieve enhanced cancer therapy through precise spatiotemporal control over drug release and efficient drug delivery to the nuclei of tumor cells.

2. EXPERIMENTAL SECTION

2.1. Synthesis and Characterization of Pu-HBSe Conjugates. 100% hydrazine monohydrate (1 mL, 25 mmol) was added dropwise into a mixture of sodium hydroxide (1.52 g, 38 mmol) and selenium powder (1.98 g, 25 mmol) in anhydrous dimethylformamide (DMF, 100 mL) at room temperature; then the mixture was vigorously stirred for 2 h. Afterward, 4-bromobenzyl (4.675 g, 25 mmol) was immersed into the reaction mixture, stirred, and refluxed at 160 °C for 4 h. After cooling to room temperature, the reaction mixture was diluted by water and extracted by ethyl acetate. The organic phase was dried by Na_2SO_4, the solvent was removed by a rotary evaporator, and the purified di-(4,1-hydroxybenzylene)diselenide (HBSe) were obtained by drying in vacuo.[37]

Carboxymethyl pullulan (CMP) was synthesized according to our previously reported methods.[27] Subsequently, CMP and EDCI were dissolved in deionized water and stirred for 30 min. Then, the solution of HBSe in DMF was added dropwise into the above mixture and stirred for 5 h. The reaction mixture was extracted with ethyl acetate, and the aqueous phase was collected. The collected mixture was dialyzed against deionized water for 24 h and lyophilized to obtain Pu-HBSe conjugates. The composition was analyzed by ^{1}H NMR (AVANCE 500, Japan) and Fourier transform infrared spectroscopy (FTIR, PerkinElmer 2000, UK).

The remaining experimental procedures could be found in the Supporting Information.

3. RESULTS AND DISCUSSION

3.1. Preparation and Characterization. In this work, a new ROS-responsive Pu-HBSe conjugate was synthesized for the first time by graft modification of HBSe containing Se−Se bond to the CMP backbone according to Figures 1 and S1. The chemical structure of the Pu-HBSe conjugate was determined by ^{1}H NMR and FTIR by comparing the peaks of CMP, HBSe, and Pu-HBSe. The Pu-HBSe ^{1}H NMR spectrum permitted the identification of the protons: 3.00−4.00 ppm (4H, glucose C2, C3, C4, and C5), 4.60−5.40 ppm (glucose, −OH), 4.82 ppm (1H, s, 1-glucose a-1,6), 5.03 ppm (1H, s, 2-glucose a-1,4), 7.18 ppm (4H, d, a-H2), and 7.45 ppm (4H, d, b-H2). The ^{1}H NMR results show the characteristic peaks of HBSe at 7−8 ppm in the Pu-HBSe spectrum (Figure S2a, Supporting Information), suggesting the successful synthesis of the conjugate, which is further validated by FTIR characterization (Figure S2b, Supporting Information). The FTIR spectra show a clear carbonyl signal at 1704 cm^{-1} in the Pu-HBSe spectrum, indicating to the successful binding of CMP to HBSe.

The Pu-HBSe conjugate with amphiphilicity self-assembled to form nanoparticles in water. A series of β-lapachone/DOX-NCS with different ratios of β-lapachone/DOX were prepared by adjusting the feed ratio of β-lapachone/DOX to nanocarriers (Table S1, Supporting Information). To strengthen the nanosystem stability and minimize the drug leakage during circulation, after loading β-lapachone/DOX, facile visible light (incandescent light bulb, 25 W, 184 Lux)-induced diselenide metathesis and regeneration[38] was employed to crosslink nanocarriers for 3 h to fabricate the core crosslinked nanosystem (β-lapachone/DOX-CCS). The high drug loading capacity of β-lapachone/DOX-CCS results from the strong π−π stacking interactions between the benzene rings in the carrier and drugs. The nanosystem with high loading capacity

DOI: 10.1021/acsami.9b15460
ACS Appl. Mater. Interfaces 2019, 11, 43581−43587

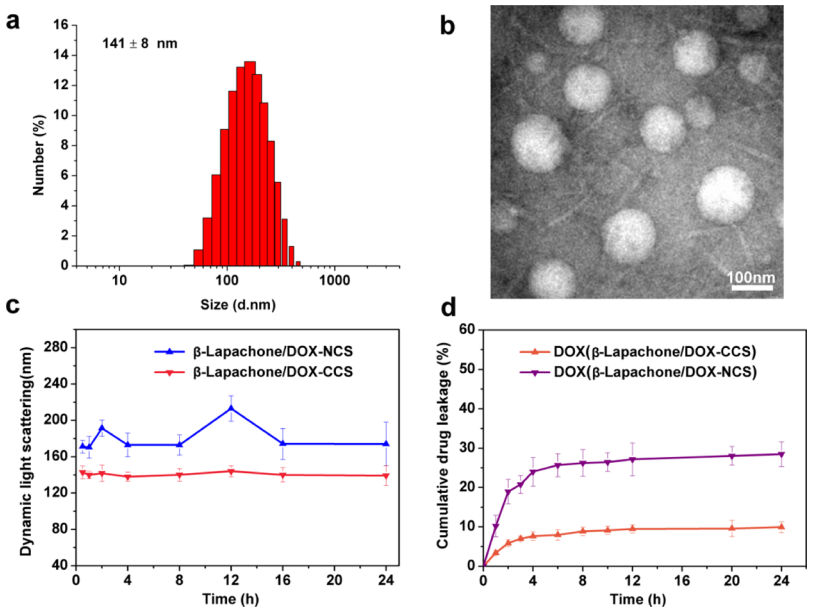

Figure 2. Characterization of β-lapachone/DOX-CCS. (a) Size distribution of β-lapachone/DOX-CCS by DLS. (b) Morphology of β-lapachone/DOX-CCS by TEM. (c) Size stability of β-lapachone/DOX-CCS at 37 °C in PBS with 10% FBS for 24 h (n = 3). (d) In vitro drug leakage from β-lapachone/DOX-CCS (n = 3).

of β-lapachone 21.6% and DOX 20.7% was chosen to assess its physicochemical properties in vitro. The morphology and size of the prepared β-lapachone/DOX-CCS were characterized using dynamic light scattering (DLS) and transmission electron microscopy (TEM). As shown in Figure 2a,b, DLS and TEM reveal that the constructed β-lapachone/DOX-CCS are spherical ones with a size around 140 nm.

To verify our hypothesis about the cross-linking design, the nanosystem stability and drug leakage were assessed. When β-lapachone/DOX-CCS was incubated in phosphate buffered saline (PBS) with 10% FBS for 24 h, the size change of the crosslinked β-lapachone/DOX-CCS was much smaller than that of the noncrosslinked β-lapachone/DOX-NCS, showing that the crosslinked β-lapachone/DOX-CCS is very stable, even in the lower concentration 1 mg/mL (Figure 2c). Furthermore, the leakage of DOX from β-lapachone/DOX-NCS and β-lapachone/DOX-CCS was compared through sealing in dialysis bags after exposing to PBS with 10% FBS (Figure 2d). β-lapachone/DOX-NCS exhibits more leakage of DOX (18.9%) compared to β-lapachone/DOX-CCS (5.4%) within 2 h, which provides evidence that the crosslinked structure would minimize the premature drug leakage and lay solid foundation for in vivo precise drug release.

To explore the drug release process, β-lapachone/DOX-CCS was exposed to different redox conditions. PBS solutions with 2 mM glutathione or 1 μM H_2O_2 were used to mimic the physiological environments of the tumor cell. PBS solutions with 100 μM H_2O_2 were used to mimic high ROS level environments after β-lapachone was catalyzed by NQO1. After 24 h incubation, 55 and 32% DOX were released in PBS solutions with 2 mM glutathione or 1 μM H_2O_2. However, in PBS solution with 100 μM H_2O_2, the DOX release dramatically increased to 75% (Figure S3, Supporting Information). These results demonstrate that the nanosystem could release a portion of DOX/β-lapachone in the presence of internal stimulants, and DOX/β-lapachone release increases as H_2O_2 concentration increases due to the breaking of the diselenide bond.

3.2. Intracellular Drug Release, Distribution, in Vitro ROS Assessments, and Synergy Study. Confocal laser scanning microscopy (CLSM) was applied to observe the subcellular drug release, distribution, and ROS generation in NQO1-overexpressing HepG2 cells (Figure 3). Because DOX acts with DNA and topoisomerase II in the nucleus, DOX

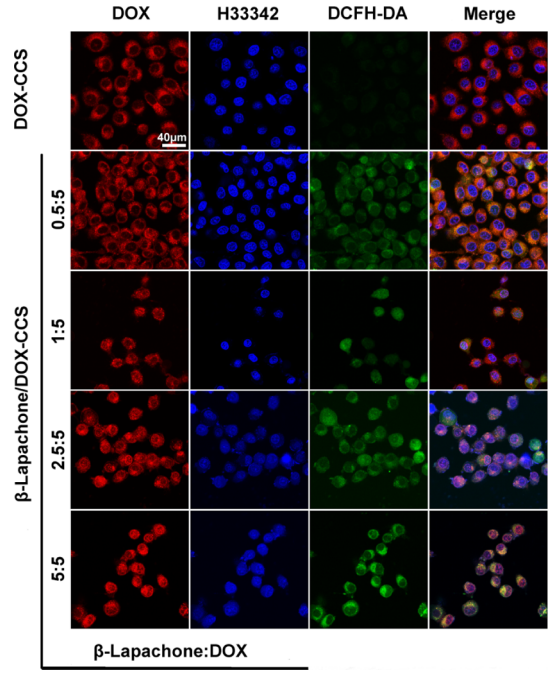

Figure 3. Intracellular DOX distribution and in vitro ROS generation after treatment. CLSM images of HepG2 cells incubated with β-lapachone/DOX-CCS at 37 °C for 4 h. [DOX concentration 10 mg/L, the proportion between DOX and β-lapachone in β-lapachone/DOX-CCS 0.5:5, 1:5, 2.5:5, and 5:5 (w/w)]. Nuclei were stained with Hoechst 33342 (blue), and ROS was stained with the DCFH-DA kit (green). The scale bar is 40 μm.

DOI: 10.1021/acsami.9b15460
ACS Appl. Mater. Interfaces 2019, 11, 43581−43587

located in the nucleus after the release is crucial to induce apoptosis. As shown in Figure 3, DOX-CCS exhibits low nuclear fluorescence at 4 h. By contrast, all β-lapachone/DOX-CCS groups have a high nuclear fluorescence, indicating more DOX release in the tumor cells. The reason is that β-lapachone could induce ROS generation through NQO1, and ROS consequently breaks Se−Se bond and release the loaded DOX. More importantly, with the increase of β-lapachone amounts in β-lapachone/DOX-CCS, the green fluorescence intensity of ROS gradually increases and the nuclear distribution of DOX increases accordingly until the nuclei is completely occupied (β-lapachone/DOX = 5:5). Average ROS fluorescence in the cells was quantitatively evaluated by flow cytometry (Figure 4b) and calculated from the CLSM images (Figure S4a,

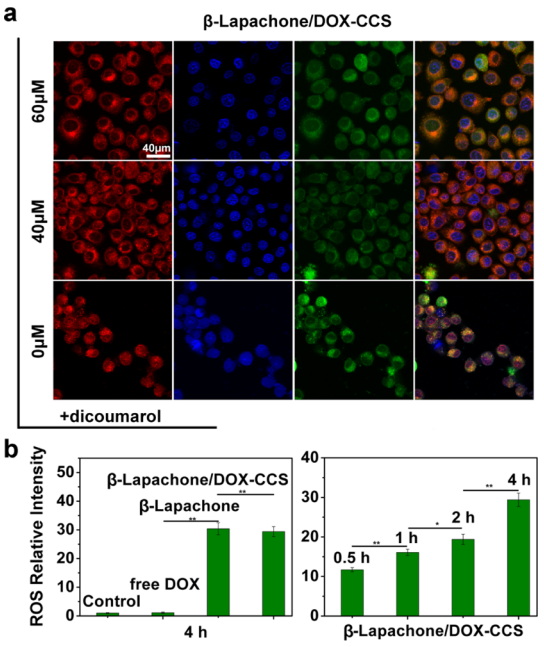

Figure 4. Intracellular DOX distribution and ROS assessments in vitro. (a) CLSM images of HepG2 cells incubated with β-lapachone/DOX-CCS and different concentrations of dicoumarol at 37 °C for 4 h (DOX concentration 10 mg/L, dicoumarol concentration 0, 40, 60 μM). (b) Flow cytometry analysis of ROS in HepG2 cells treated with DOX, β-lapachone, or β-lapachone/DOX-CCS (DOX concentration 9.58 mg/L, β-lapachone concentration 10 mg/L). The scale bar is 40 μm.

Supporting Information). The difference between different β-lapachone amounts in terms of the DOX fluorescence from β-lapachone/DOX-CCS within the nucleus indicates that β-lapachone generates abundant exogenous-stimulant ROS via NQO1 catalysis and plays a crucial role in the drug release. These results confirm our previous hypothesis about the design of this nanosystem.

To manifest the effect of drug release triggered by ROS via NQO1 catalysis, the NQO1 competitive inhibitor dicoumarol was subsequently introduced for the retrospective method. Average ROS fluorescence in the cells and DOX fluorescence in the cell nuclei were calculated from the CLSM images (Figure S4, Supporting Information). The nuclear fluorescence of DOX from β-lapachone/DOX-CCS increases progressively with decreasing amounts of dicoumarol (60, 40, 0 μM) (Figures 4a, S4d, Supporting Information), which further confirms that abundant exogenous-stimulant ROS via NQO1 catalysis is important to the cascade drug release.

We investigated the efficiency of β-lapachone-induced ROS generation in the HepG2 cells. Cells treated with free DOX (9.58 mg/L), β-lapachone (10 mg/L), or β-lapachone/DOX-CCS (β-lapachone 10 mg/L and DOX 9.58 mg/L) were analyzed by a flow cytometer (Figure 4b). β-Lapachone and β-lapachone/DOX-CCS significantly enhances ROS concentration as the incubation time prolongs. Nevertheless, DOX barely elevates the intracellular ROS concentration. At 4 h, ROS fluorescence increases by ∼30 times, and β-lapachone/DOX-CCS produces a similar amount of ROS as free β-lapachone, suggesting a high intracellular ROS level.

The combination index (CI) of β-lapachone and DOX was calculated by Chou−Talalay method (Table S2). CI values were <1, thus suggesting the synergistic effect of β-lapachone and DOX.

3.3. In Vivo Pharmacokinetic Study, Biodistribution, and Intratumoral Release. The in vivo pharmacokinetics of β-lapachone/DOX-CCS has been conducted. As shown in Figure S5, after 24 h, 9.4% of β-lapachone/DOX-CCS was in the plasma compared with 0.3% of free DOX and 5.7% β-lapachone/DOX-NCS. β-Lapachone/DOX-CCS displayed longer blood circulation time.

To explore the tumor-targeting of the nanosystem, in vivo distribution of β-lapachone/DOX-CCS in HepG2-xenografted mice was systematically studied after injection of β-lapachone/DOX-CCS at a dose of 10 mg kg^{-1} for obtaining a clear imaging effect within a safe limit. The in vivo imaging of mice was conducted at 8, 12, and 24 h postinjection by the PerkinElmer IVIS Lumina III Imaging System. As shown in Figure 5a, more DOX fluorescence of β-lapachone/DOX-CCS is observed to locate on the tumor tissue at 8 h compared with free DOX and β-lapachone/DOX-NCS (Figure S6, Supporting

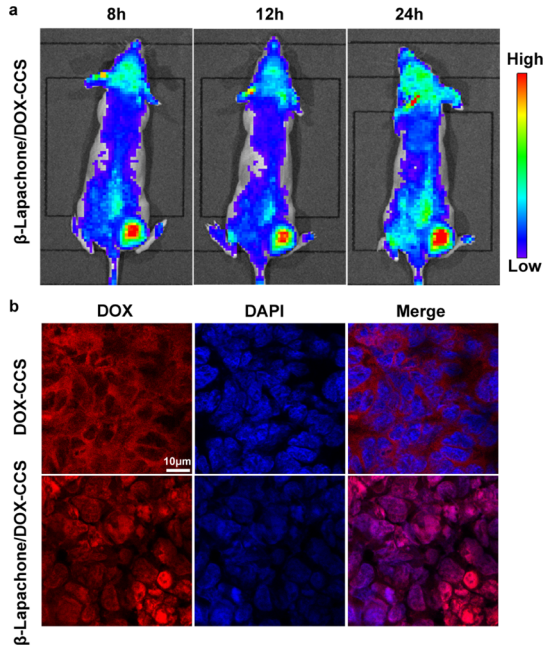

Figure 5. In vivo drug accumulation. (a) In vivo optical fluorescence imaging of mice-bearing HepG2-induced tumor with β-lapachone/DOX-CCS for 8, 12, and 24 h postinjection (10 mg/kg of DOX). (b) CLSM images of the HepG2-induced tumor cryosections at 24 h postinjection of β-lapachone/DOX-CCS. The scale bar is 10 μm.

DOI: 10.1021/acsami.9b15460
ACS Appl. Mater. Interfaces 2019, 11, 43581−43587

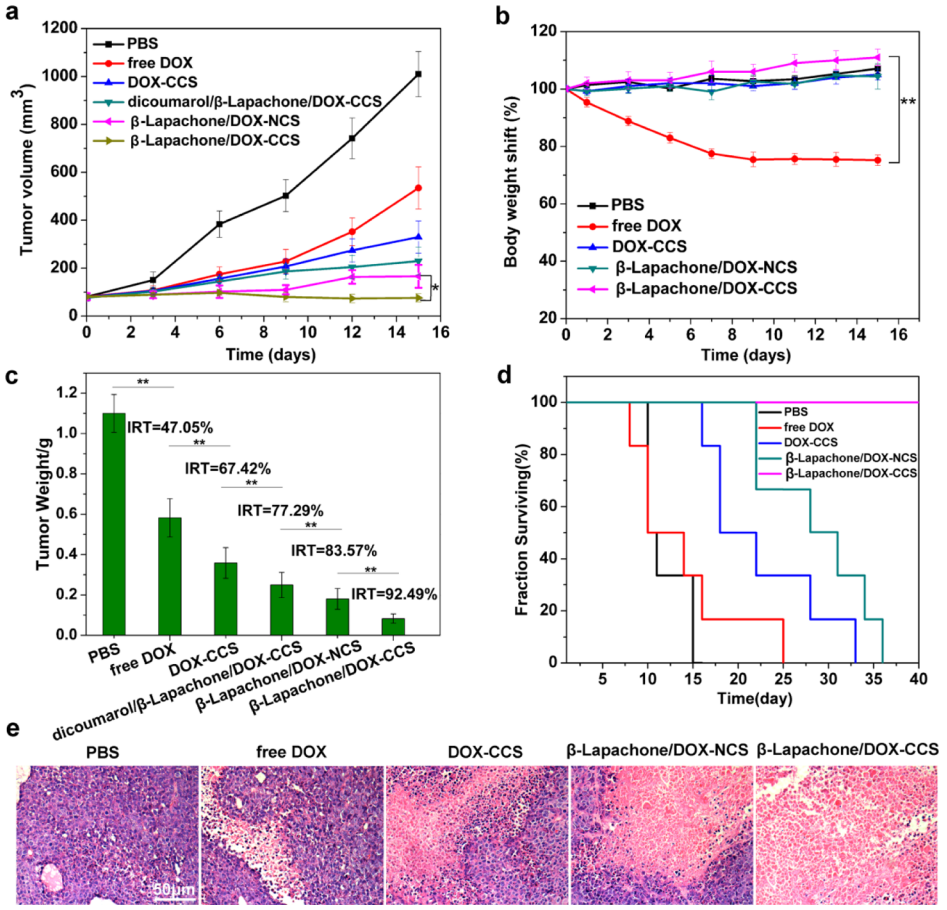

Figure 6. In vivo antitumor effect. (a) Tumor inhibition curves, (b) body weight change, (c) tumor weight, (d) survival rates, and (e) histological observation of nude mice bearing HepG2-induced tumors administrated with PBS, free DOX, DOX-CCS, β-lapachone/DOX-NCS, dicoumarol/β-lapachone/DOX-CCS, and β-lapachone/DOX-CCS (DOX dosage: 5 mg/kg body weight). Data were presented as mean ± standard deviation by *t*-test, $*p < 0.05$, $**p < 0.01$. The scale bar is 50 μm.

Information). Moreover, β-lapachone/DOX-CCS performs lasting fluorescence at the tumor 24 h, suggesting the long circulation and excellent tumor-targeting of the nanoparticles at the tumor site. Quantification of DOX distribution in the tumors was also conducted by the tissue distribution method (Figure S7, Supporting Information). DOX in the tumor tissue reaches as high as 16.7% of the injected dose, which is even higher than that in the reticuloendothelial system such as liver and spleen responsible for the clearance of exogenous nanoparticles and kidney for excretion. The result demonstrates that the crosslinked nanoparticles could greatly improve the in vivo tumor-targeting property through preventing premature drug leakage, which offers opportunity for loaded drug to accumulate in the tumor tissue.

To clearly observe the intratumoral release and distribution of DOX in the tumor cell, a portion of tumors were collected at 24 h and CLSM imaging displayed a precise location of DOX (Figure 5b). Average DOX fluorescence in the cell nuclei was calculated from the CLSM images (Figure S8, Supporting Information). The images show that DOX signals of the β-lapachone/DOX-CCS group in the cell nuclei are remarkably stronger than that of DOX-CCS group. This result reveals that β-lapachone could greatly increase the release efficacy and delivery to the nuclei of tumor cells of DOX from β-lapachone/DOX-CCS in the tumor cells.

3.4. Antitumor Efficacy. The above results demonstrate that the enzyme-catalytic self-triggered release of the drug from the nanosystem is meaningful for tumor therapy at the cellular level. To show the potential of β-lapachone/DOX-CCS in vivo, the antitumor efficacy of β-lapachone/DOX-CCS was assessed in HepG2-xenografted nude mice. Mice-bearing tumors of 80 mm^3 were divided into six groups for the treatment administered. As shown in Figure 6a,c, the inhibition rate of tumor growth (IRT) for β-lapachone/DOX-CCS is 92.49%, which is obviously higher than the 47.05% of free DOX, 67.42% of DOX-CCS, 77.29% of dicoumarol/β-lapachone/DOX-CCS, and 83.57% of β-lapachone/DOX-NCS. β-lapachone/DOX-CCS shows higher efficacy on inhibiting the tumor growth compared with β-lapachone/DOX-NCS, which verifies that the crosslinked nanoparticles could improve the in vivo tumor-targeting property. Compared with DOX-CCS and dicoumarol/β-lapachone/DOX-CCS, β-lapachone/DOX-CCS shows better efficacy in inhibiting the tumor growth, which further suggests that sufficient drug release, efficient drug delivery to the nuclei of tumor cells, and the synergy of DOX and ROS on tumor suppression are well fulfilled by β-lapachone/DOX-CCS. Therefore, β-lapachone and cross-linking could significantly influence characteristics of the nanosystem and their biological fate in vivo.

To further evaluate the therapeutic efficacy, the excised tumors were processed for hematoxylin and eosin (H&E) (Figure 6e). The treatment of β-lapachone/DOX-CCS results in the highest level of cell apoptosis in the tumor tissue, which is superior to that of free DOX, DOX-CCS, and β-lapachone/

DOI: 10.1021/acsami.9b15460
ACS Appl. Mater. Interfaces 2019, 11, 43581−43587

DOX-NCS groups. In groups treated with free DOX, cardiomyocyte nuclear lysis and glomerular pyknosis were observed in the heart and kidney (Figure S9). In contrast, β-lapachone/DOX-CCS resulted in no obvious damage, suggesting that β-lapachone/DOX-CCS could reduce drug toxicity.

The survival rate of mice treated with different formulas was also investigated (Figure 6d). Mice treated with β-lapachone/DOX-CCS survive over 50 d. Mice treated with PBS, free DOX, DOX-CCS, and β-lapachone/DOX-NCS do not survive over 15, 25, 33, and 36 d, respectively. Moreover, the average body weights of all groups at the end point changed by <15.0% while about 25.0% weight loss is observed in the free DOX group (Figure 6b), suggesting negligible side effects of β-lapachone/DOX-CCS. The safety of β-lapachone/DOX-CCS might be related to the NQO1 enzyme besides cross-linking. The low expression of the NQO1 enzyme in the normal cells results in the lower release of DOX from β-lapachone/DOX-CCS.

Overall, the synergistic functions of β-lapachone/DOX-CCS, including precise drug delivery to the nuclei of tumor cells, oxidative cytotoxicity of ROS, and combined chemotherapy of DOX and β-lapachone, were demonstrated to improve tumor inhibition efficacy with reduced adverse effects. Based on the safety and efficiency of β-lapachone/DOX-CCS, it might serve as a new direction and lead us to further research for clinical cancer therapy.

4. CONCLUSIONS

In summary, a core crosslinked nanosystem (β-lapachone/DOX-CCS), which could self-trigger release of a loaded drug via enzyme catalysis, has been successfully constructed by the encapsulation of β-lapachone. The research results reveal that the crosslinked β-lapachone/DOX-CCS is able to achieve efficient drug delivery to the nuclei of tumor cells and improve tumor inhibition efficacy with reduced adverse effects. Therefore, this research might provide new possibilities in developing effective yet green cancer therapy paradigms.

■ ASSOCIATED CONTENT

Supporting Information

The Supporting Information is available free of charge on the ACS Publications website at DOI: 10.1021/acsami.9b15460.

Chemical equation; FTIR and ^{1}H NMR characterizations of CMP, HBSe and Pu-HBSe, drug loading content, particle size and DOX releases of β-lapachone/DOX-CCS, CI of DOX/β-lapachone, average ROS fluorescence in the cells and DOX fluorescence in the cell nuclei calculated from CLSM images, in vivo pharmacokinetics, in vivo optical fluorescence imaging, and DOX biodistribution and histological observation (PDF)

■ AUTHOR INFORMATION

Corresponding Authors

*E-mail: 102733@cqmu.edu.cn (H.L.).
*E-mail: gangliu.cmitm@xmu.edu.cn (G.L.).
*E-mail: lifq@cqmu.edu.cn (F.L.).

ORCID

Huanan Li: 0000-0003-1727-2937
Deping Zeng: 0000-0003-3843-8297
Gang Liu: 0000-0003-2613-7286

Notes

The authors declare no competing financial interest.

■ ACKNOWLEDGMENTS

This project was financially supported by Chongqing Research Program of Basic Research and Frontier Technology (no. cstc2019jcyj-msxmX0334 to H.L.) and National Natural Science Foundation of China (no. 11574039 to F.L.).

■ REFERENCES

(1) Peer, D.; Karp, J. M.; Hong, S.; Farokhzad, O. C.; Margalit, R.; Langer, R. Nanocarriers as an emerging platform for cancer therapy. *Nat. Nanotechnol.* **2007**, *2*, 751−760.

(2) Torchilin, V. P. Multifunctional, stimuli-sensitive nanoparticulate systems for drug delivery. *Nat. Rev. Drug Discov.* **2014**, *13*, 813−827.

(3) Xu, X.; Ho, W.; Zhang, X.; Bertrand, N.; Farokhzad, O. Cancer nanomedicine: from targeted delivery to combination therapy. *Trends Mol. Med.* **2015**, *21*, 223−232.

(4) Bertrand, N.; Wu, J.; Xu, X.; Kamaly, N.; Farokhzad, O. C. Cancer nanotechnology: the impact of passive and active targeting in the era of modern cancer biology. *Adv. Drug Deliv. Rev.* **2014**, *66*, 2−25.

(5) Oude Blenke, E.; Mastrobattista, E.; Schiffelers, R. M. Strategies for triggered drug release from tumor targeted liposomes. *Expert Opin. Drug Deliv.* **2013**, *10*, 1399−1410.

(6) Wang, Y.; Wei, G.; Zhang, X.; Xu, F.; Xiong, X.; Zhou, S. A Step-by-Step Multiple Stimuli-Responsive Nanoplatform for Enhancing Combined Chemo-Photodynamic Therapy. *Adv. Mater.* **2017**, *29*, 1605357.

(7) Mura, S.; Nicolas, J.; Couvreur, P. Stimuli-responsive nanocarriers for drug delivery. *Nat. Mater.* **2013**, *12*, 991−1003.

(8) Chen, C.; Geng, J.; Pu, F.; Yang, X.; Ren, J.; Qu, X. Polyvalent nucleic acid/mesoporous silica nanoparticle conjugates: dual stimuli-responsive vehicles for intracellular drug delivery. *Angew Chem. Int. Ed. Engl.* **2011**, *50*, 882−886.

(9) Ye, Z.; Wu, W.-R.; Qin, Y.-F.; Hu, J.; Liu, C.; Seeberger, P. H.; Yin, J. An integrated therapeutic delivery system for enhanced treatment of hepatocellular carcinoma. *Adv. Funct. Mater.* **2018**, *28*, 1706600.

(10) Wang, Y.; Wei, G.; Zhang, X.; Huang, X.; Zhao, J.; Guo, X.; Zhou, S. Multistage Targeting Strategy Using Magnetic Composite Nanoparticles for Synergism of Photothermal Therapy and Chemotherapy. *Small* **2018**, *14*, 1702994.

(11) Naz, S.; Wang, M.; Han, Y.; Hu, B.; Teng, L.; Zhou, J.; Zhang, H.; Chen, J. Enzyme-responsive mesoporous silica nanoparticles for tumor cells and mitochondria multistage-targeted drug delivery. *Int. J. Nanomed.* **2019**, *14*, 2533−2542.

(12) Huang, P.; Chen, Y.; Lin, H.; Yu, L.; Zhang, L.; Wang, L.; Zhu, Y.; Shi, J. Molecularly organic/inorganic hybrid hollow mesoporous organosilica nanocapsules with tumor-specific biodegradability and enhanced chemotherapeutic functionality. *Biomaterials* **2017**, *125*, 23−37.

(13) Liu, Z.; Chen, X.; Zhang, X.; Gooding, J. J.; Zhou, Y. Carbon-Quantum-Dots-Loaded Mesoporous Silica Nanocarriers with pH-Switchable Zwitterionic Surface and Enzyme-Responsive Pore-Cap for Targeted Imaging and Drug Delivery to Tumor. *Adv. Healthc. Mater.* **2016**, *5*, 1401−1407.

(14) Chen, X.; Liu, Z.; Parker, S. G.; Zhang, X.; Gooding, J. J.; Ru, Y.; Liu, Y.; Zhou, Y. Light-Induced Hydrogel Based on Tumor-Targeting Mesoporous Silica Nanoparticles as a Theranostic Platform for Sustained Cancer Treatment. *ACS Appl. Mater. Interfaces* **2016**, *8*, 15857−15863.

(15) Wang, C.; Chen, S.; Wang, Y.; Liu, X.; Hu, F.; Sun, J.; Yuan, H. Lipase-Triggered Water-Responsive "Pandora's Box" for Cancer Therapy: Toward Induced Neighboring Effect and Enhanced Drug Penetration. *Adv. Mater.* **2018**, *30*, 1706407.

DOI: 10.1021/acsami.9b15460
ACS Appl. Mater. Interfaces 2019, 11, 43581−43587

(16) Ke, C.-J.; Su, T.-Y.; Chen, H.-L.; Liu, H.-L.; Chiang, W.-L.; Chu, P.-C.; Xia, Y.; Sung, H.-W. Smart multifunctional hollow microspheres for the quick release of drugs in intracellular lysosomal compartments. *Angew Chem. Int. Ed. Engl.* **2011**, *50*, 8086−8089.
(17) Heidarli, E.; Dadashzadeh, S.; Haeri, A. State of the Art of Stimuli-Responsive Liposomes for Cancer Therapy. *Iran. J. Pharm. Res.* **2017**, *16*, 1273−1304.
(18) Yang, Y.; Lu, Y.; Abbaraju, P. L.; Azimi, I.; Lei, C.; Tang, J.; Jambhrunkar, M.; Fu, J.; Zhang, M.; Liu, Y.; Liu, C.; Yu, C. Stepwise degradable nanocarriers enabled cascade delivery for synergistic cancer therapy. *Adv. Funct. Mater.* **2018**, *28*, 1800706.
(19) Ma, X.; Huang, X.; Moore, Z.; Huang, G.; Kilgore, J. A.; Wang, Y.; Hammer, S.; Williams, N. S.; Boothman, D. A.; Gao, J. Esterase-activatable beta-lapachone prodrug micelles for NQO1-targeted lung cancer therapy. *J. Control. Release* **2015**, *200*, 201−211.
(20) Wu, Y.; Wang, X.; Chang, S.; Lu, W.; Liu, M.; Pang, X. beta-Lapachone Induces NAD(P)H:Quinone Oxidoreductase-1- and Oxidative Stress-Dependent Heat Shock Protein 90 Cleavage and Inhibits Tumor Growth and Angiogenesis. *J. Pharmacol. Exp. Ther.* **2016**, *357*, 466−475.
(21) Ye, M.; Han, Y.; Tang, J.; Piao, Y.; Liu, X.; Zhou, Z.; Gao, J.; Rao, J.; Shen, Y. A Tumor-Specific Cascade Amplification Drug Release Nanoparticle for Overcoming Multidrug Resistance in Cancers. *Adv. Mater.* **2017**, *29*, 1702342.
(22) Guhagarkar, S. A.; Gaikwad, R. V.; Samad, A.; Malshe, V. C.; Devarajan, P. V. Polyethylene sebacate-doxorubicin nanoparticles for hepatic targeting. *Int. J. Pharm.* **2010**, *401*, 113−122.
(23) Yim, H.; Yang, S.-G.; Jeon, Y. S.; Park, I. S.; Kim, M.; Lee, D. H.; Bae, Y. H.; Na, K. The performance of gadolinium diethylene triamine pentaacetate-pullulan hepatocyte-specific T1 contrast agent for MRI. *Biomaterials* **2011**, *32*, 5187−5194.
(24) Rekha, M. R.; Sharma, C. P. Blood compatibility and in vitro transfection studies on cationically modified pullulan for liver cell targeted gene delivery. *Biomaterials* **2009**, *30*, 6655−6664.
(25) Li, H.; Yu, C.; Zhang, J.; Li, Q.; Qiao, H.; Wang, Z.; Zeng, D. pH-sensitive pullulan-doxorubicin nanoparticles loaded with 1,1,2-trichlorotrifluoroethane as a novel synergist for high intensity focused ultrasound mediated tumor ablation. *Int. J. Pharm.* **2019**, *556*, 226−235.
(26) Li, H.; Sun, Y.; Liang, J.; Fan, Y.; Zhang, X. pH-Sensitive pullulan-DOX conjugate nanoparticles for co-loading PDTC to suppress growth and chemoresistance of hepatocellular carcinoma. *J. Mater. Chem. B* **2015**, *3*, 8070−8078.
(27) Li, H.; Cui, Y.; Sui, J.; Bian, S.; Sun, Y.; Liang, J.; Fan, Y.; Zhang, X. Efficient Delivery of DOX to Nuclei of Hepatic Carcinoma Cells in the Subcutaneous Tumor Model Using pH-Sensitive Pullulan-DOX Conjugates. *ACS Appl. Mater. Interfaces* **2015**, *7*, 15855−15865.
(28) Li, H.; Cui, Y.; Liu, J.; Bian, S.; Liang, J.; Fan, Y.; Zhang, X. Reduction breakable cholesteryl pullulan nanoparticles for targeted hepatocellular carcinoma chemotherapy. *J. Mater. Chem. B* **2014**, *2*, 3500−3510.
(29) Li, H.; Ma, M.; Zhang, J.; Hou, W.; Chen, H.; Zeng, D.; Wang, Z. Ultrasound-Enhanced Delivery of Doxorubicin-Loaded Nanodiamonds from Pullulan-all-trans-Retinal Nanoparticles for Effective Cancer Therapy. *ACS Appl. Mater. Interfaces* **2019**, *11*, 20341−20349.
(30) Huang, L.; Chaurasiya, B.; Wu, D.; Wang, H.; Du, Y.; Tu, J.; Webster, T. J.; Sun, C. Versatile redox-sensitive pullulan nanoparticles for enhanced liver targeting and efficient cancer therapy. *Nanomedicine* **2018**, *14*, 1005−1017.
(31) Sui, J.; Cui, Y.; Cai, H.; Bian, S.; Xu, Z.; Zhou, L.; Sun, Y.; Liang, J.; Fan, Y.; Zhang, X. Synergistic chemotherapeutic effect of sorafenib-loaded pullulan-Dox conjugate nanoparticles against murine breast carcinoma. *Nanoscale* **2017**, *9*, 2755−2767.
(32) Read, E. S.; Armes, S. P. Recent advances in shell cross-linked micelles. *Chem. Commun.* **2007**, 3021−3035.
(33) Zhai, S.; Hu, X.; Hu, Y.; Wu, B.; Xing, D. Visible light-induced crosslinking and physiological stabilization of diselenide-rich nanoparticles for redox-responsive drug release and combination chemotherapy. *Biomaterials* **2017**, *121*, 41−54.
(34) Zhao, Q.; Yang, X. L.; Holtzclaw, W. D.; Talalay, P. Unexpected genetic and structural relationships of a long-forgotten flavoenzyme to NAD(P)H:quinone reductase (DT-diaphorase). *Proc. Natl. Acad. Sci. U.S.A.* **1997**, *94*, 1669−1674.
(35) Chau, Y.-P.; Shiah, S.-G.; Don, M.-J.; Kuo, M.-L. Involvement of hydrogen peroxide in topoisomerase inhibitor beta-lapachone-induced apoptosis and differentiation in human leukemia cells. *Free Radical Biol. Med.* **1998**, *24*, 660−670.
(36) Samali, A.; Nordgren, H.; Zhivotovsky, B.; Peterson, E.; Orrenius, S. A comparative study of apoptosis and necrosis in HepG2 cells: oxidant-induced caspase inactivation leads to necrosis. *Biochem. Biophys. Res. Commun.* **1999**, *255*, 6−11.
(37) Rizvi, M. A.; Guru, S.; Naqvi, T.; Kumar, M.; Kumbhar, N.; Akhoon, S.; Banday, S.; Singh, S. K.; Bhushan, S.; Mustafa Peerzada, G.; Shah, B. A. An investigation of in vitro cytotoxicity and apoptotic potential of aromatic diselenides. *Bioorg. Med. Chem. Lett.* **2014**, *24*, 3440−3446.
(38) Ji, S.; Cao, W.; Yu, Y.; Xu, H. Visible-Light-Induced Self-Healing Diselenide-Containing Polyurethane Elastomer. *Adv. Mater.* **2015**, *27*, 7740−7745.

DOI: 10.1021/acsami.9b15460
ACS Appl. Mater. Interfaces 2019, 11, 43581−43587